New constraints on metamorphic history of Adirondack diopsides (New York, U.S.A.): Al and $\delta^{18}O$ profiles

G. Desbois,[1] J. Ingrin,[1,*] N.T. Kita,[2] J.W. Valley,[2] and E. Deloule[3]

[1]Minéralogie, LMTG-CNRS-OMP—Université Paul Sabatier, 14 Avenue Edouard Belin, F-31400 Toulouse, France
[2]Department of Geology and Geophysics, University of Wisconsin, Madison, Wisconsin 53706, U.S.A.
[3]CRPG-CNRS, BP20, F-54501 Vandoeuvre Cedex, France

ABSTRACT

Detailed electron- and ion-microprobe analysis of diopsides extracted from a block of marble collected in the Mt. Marcy anorthosite massif (Adirondack Highlands, New York) shows that single crystals have preserved Al-Si zoning features from early contact metamorphism later modified by regional metamorphism. Diopsides show Al and Si complementary zoning from core to rim; average Al concentration in rims is constant (0.11 pfu), but values in the cores vary with crystals from 0.06 to 0.14 pfu. A $\delta^{18}O$ profile measured with the ion microprobe shows no zoning. Modeling of the Al-diffusion profiles affected by regional metamorphism of the Grenville orogeny shows that original Al zoning was sharp and corresponds to a rapid change of crystal-growth conditions during early contact metamorphism: (1) diopside cores crystallized with variable Al contents due to restricted fluid circulation or differing sedimentary composition, (2) then pervasive fluid infiltration crystallized the homogeneous rim of diopside, and (3) core to rim Al zoning was later smoothed by granulite-facies metamorphism. Homogeneity of $\delta^{18}O$ in core and mantle (near rim) of diopsides suggests that the crystals were isotopically homogeneous prior to and during regional metamorphism. Values of Al-Si diffusion coefficient deduced from modeling are in agreement with low-temperature extrapolation of experimental data.

Keywords: Diopside, zoning, granulite, diffusion, ion probe, oxygen isotopes, Adirondack

INTRODUCTION

Zonation in minerals can be used to determine the duration of metamorphic events or the cooling rate of rocks (Dodson 1973; Lasaga 1983; Farver 1989; Eiler et al. 1992, 1993; Valley 2001). Diopsides collected in a marble xenolith from the Adirondack Highlands (New York) are ideal to perform such analyses (Edwards and Valley 1998). Several authors (Sharp and Jenkin 1994; Edwards and Valley 1998; Johnson et al. 2002; Jaoul and Béjina 2005) have explored the O- and H-diffusion process occurring in diopsides from the Adirondack Highlands but studies on possible zonations of other elements are lacking. One objective of this paper is to check if diopsides have preserved chemical zoning of major elements like Mg, Al, Fe, and Si recording the complex polymetamorphic history of the Adirondack Highlands. Previous O-isotope studies were based on bulk-mineral measurements of $\delta^{18}O$ performed in different grain sizes, and the authors assumed that samples had been isotopically homogenized by the last high-temperature metamorphism (granulite facies) before cooling (Eiler et al. 1995; Edwards and Valley 1998). Another objective of this paper is to check the validity of this assumption.

In this paper, we performed detailed electron-microprobe analyses and in situ ion-probe $\delta^{18}O$ measurements in diopside single crystals from the Adirondack Highlands. Results are compared with known metamorphic history, and analyzed using diffusion data in diopside (Farver 1989; Elphick and Graham 1990; Jaoul et al. 1991; Ryerson and McKeegan 1994; Sharp and Jenkin 1994; Béjina and Jaoul 1996; Pacaud et al. 1999; Ingrin et al. 2001).

MATERIALS AND METHODS

Samples

Three diopside single crystals (1.1, 1.2, 1.3) were selected from a single block of marble located in the Cascade Slide xenolith in the Mt. Marcy quadrangle, in the Central Adirondack Highlands (Fig. 1). These crystals are from sample 1 of Edwards and Valley (95ADK-1 1998). The marble forms a metasedimentary xenolith or pendant in the Mt. Marcy anorthosite massif (Valley and Essene 1980).

Diopside grains were extracted from the calcite matrix by HCl dissolution. Samples have been selected for their relative lack of cracks and inclusions, and apparent purity. Thin sections were cut either parallel or perpendicular to the [001] axis through the middle of the crystal (Table 1). The orientation of the crystals was determined by measurement of the angle between crystal faces with an optical theodolite goniometer, and the orientation of the sample 1.1 was confirmed by single-crystal X-ray precession photography. Direction [001] corresponds systematically to the longest direction of crystal growth. Samples were embedded in epoxy and polished down to the 4000 grit with SiC paper, and then down to 0.3 μm with Al_2O_3 powder. Samples have a composition close to pure diopside (Table 1).

Metamorphic history experienced by diopside samples

As diopside samples were collected from the Cascade Slide Xenolith, a block of marble within the Mt. Marcy anorthosite massif (Fig. 1), thermal history experienced by these samples is closely linked to the thermal history of the anorthosite massif. The intrusion of anorthosite and related rocks of the AMCG suite (anorthosite, mangerite, charnockite, granite) occurred at 1155 ± 5 Ma at shallow crustal levels (Clechenko and Valley 2003; McLelland et al. 2004). The temperature of the anorthosite crystallization was ca. 1100 °C (Bohlen and Essene 1978). U-Pb geochronology on zircon, garnet, sphene, monazite, and rutile (McLelland et al. 1988, 1996, 2001, 2004; Mezger et al. 1991) shows that this portion of the Grenville province experienced regional granulite-facies metamorphism around

1050 Ma during the Ottawan stage of the Grenville orogenic cycle. Temperature and pressure of the granulite-facies metamorphism at the sample location are respectively 770 ± 30 °C and 7–8 kbar (Bohlen et al. 1985) and lasted for around 50 Ma (Mezger et al. 1991; McLelland et al. 2001). For the Central Adirondack Highlands, the cooling was slow, 1 to 4 K/Ma during the 200 Ma after the peak of metamorphism (Mezger et al. 1991; Jaoul and Béjina 2005).

Fluid conditions in the Adirondack Highlands evolved over the polymetamorphic history of the region. During early, relatively shallow contact metamorphism adjacent to the anorthosite massif, marbles were generally fluid saturated. Locally, flow of hydrothermal fluids caused extensive metasomatism, as evidenced by massive wollastonite skarns at Willsboro and elsewhere (Clechenko and Valley 2003). Later, after burial and reheating, conditions were fluid absent for most rocks during granulite-facies metamorphism. The marbles and calc-silicates in the Cascade Slide xenolith contain many minerals formed during contact metamorphism under fluid-present conditions, including wollastonite, monticellite, and akermanite (Valley and Essene 1980), that were subsequently preserved during regional granulite-facies conditions because of fluid-absent conditions (i.e., low f_{H_2O} and low f_{CO_2}).

Analytical techniques

The chemical compositions of diopside crystals 1.1, 1.2, and 1.3 were determined using the SX50 CAMECA electron microprobe at the Université Paul Sabatier, Toulouse, operating at 15 kV and 20 nA with a nominal spot size of 3 μm in diameter. The following standards were used: Si (wollastonite), Ti ($MnTiO_3$), Al (corundum), Cr (Cr_2O_3), Fe (Fe_2O_3), Mn ($MnTiO_3$), Mg (MgO), Ca (wollastonite), Na (albite), and K (sanidine). Samples have been analyzed from edge to edge along main crystallographic directions defined in Table 1. For all profile measurements, mean distance between each analytical point is 7 μm. The Al map for sample 1.1 is a compilation of 421 analyses with an average spacing of 50 μm (Fig. 2).

Oxygen-isotope measurements have been performed by CAMECA IMS-1280 ion microprobe at the University of Wisconsin-Madison. For these analyses, the samples were coated with a gold thin film and charge neutralization was aided by an electron flood gun. The primary ion beam was $^{133}Cs^+$ and secondary ions of O$^-$ were analyzed using two Faraday cups in multi-collector mode. A primary beam current of ~3 nA yielded 3×10^9 cps on ^{16}O and 6×10^6 cps on ^{18}O. The spot diameter was about 15 μm. A mass-resolving power of 2500 was sufficient to remove hydride interferences on mass 18. Low-energy ions were analyzed with an energy window of 40 eV. Before each analysis, the secondary beam was aligned to a 4000 μm field aperture, which collimates a 20×20 μm square area surrounding the analysis spot on the sample surface using a transfer lens magnification of 200×. Each analysis consisted of a total integrating time of 80 s, and the total time for each analysis was less than 5 minutes. Isotope ratios are presented in standard per mil format relative to VSMOW, and 1σ internal errors on each spot are close to 0.1‰. The strategy of analysis was to use the homogeneous core of the diopside crystal as a standard ($\delta^{18}O$ = 23.04‰ VSMOW, Edwards and Valley 1998). The spot to spot reproducibility of 17 standard analyses (1 std. dev. = 0.10‰, 1 std. err. = 0.024‰) match the internal error (Table 2). Analyses were performed along a ~600 μm traverse parallel to [001] from the mantle to the center of crystal, and three standard analyses were made bracketing every three sample spots (Fig. 3a). Raw data for the center of the diopside crystal drifted by ~0.01‰ per analysis over the period of 32 analyses. Data were corrected for linear instrument drift and instrumental mass fractionation of +5.6‰, and are reported in standard per mil notation relative to VSMOW. The results are plotted as a function of distance to the crystal boundary in Figure 3b.

An FTIR analysis performed on crystal 1.1 shows that only one OH band at 3645 cm^{-1} is present, as was reported by Johnson et al. (2002) for a different crystal of diopside from the same hand sample.

RESULTS

Aluminum, silicon profiles

Major-element profiles have been measured with the electron microprobe for the three samples. Aluminum, Si, Mg, and Fe analyses show cation zoning. Figure 2 shows profiles from the sample 1.1 measured along [100]*. Concentrations for six O atoms are plotted as a function of position from edge to edge. The profiles highlight solid solution of Al and Si in diopside weakly
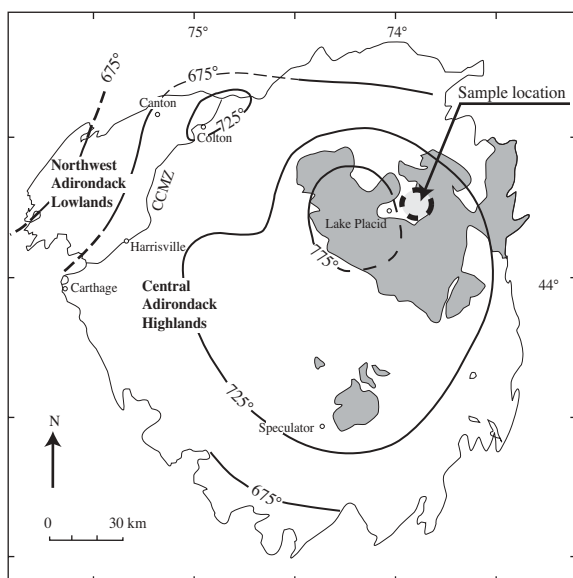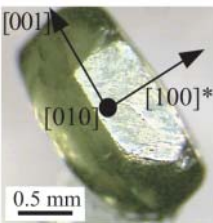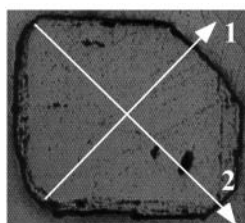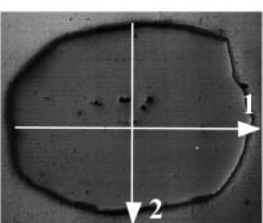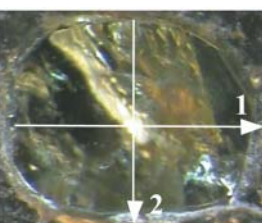

FIGURE 1. Sample location in the Adirondack Mountains (New York). The figure shows isotherms of granulite facies metamorphism in the central Adirondack Highlands and amphibolite facies in the Northwest Adirondack Lowlands based on two feldspars and Fe-Ti oxide thermometry (Bohlen et al. 1985) and $\Delta^{13}C_{Calcite—graphite}$ measurements (Kitchen and Valley 1995). Regions in gray are anorthosite. The sample is the same as sample 1 (95ADK-1) of Edwards and Valley (1998).

TABLE 1. Diopside samples: Image of crystals 1.1, 1.2, and 1.3; optical thin section with reflected light, orientations, size, and mean composition

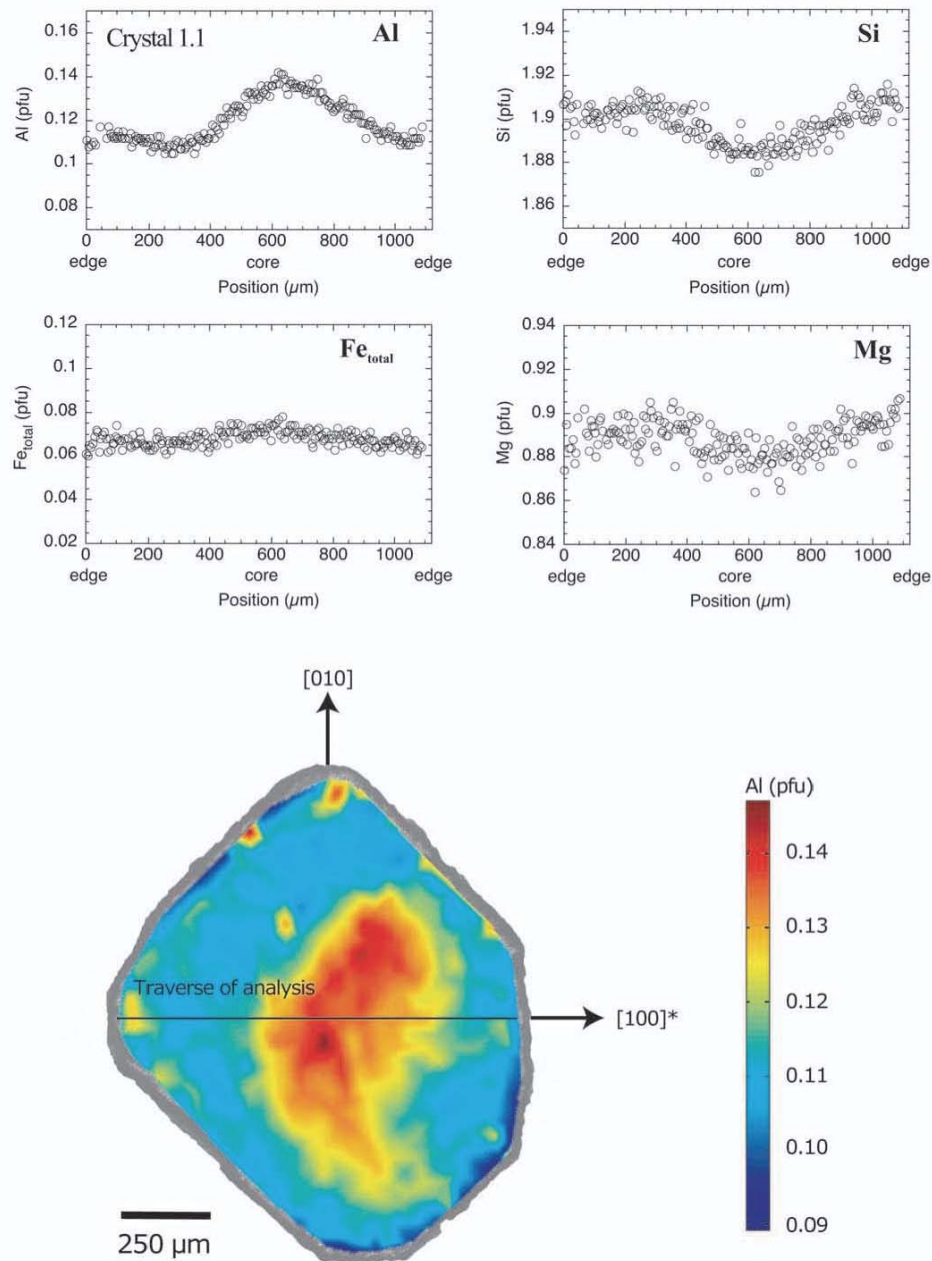| Thin sections		Crystal 1.1	Crystal 1.2	Crystal 1.3
Directions	1:	[100]*	[001]	[001]
	2:	[010]	~[110]*	unknown
Length	1:	1.18 mm	1.91 mm	1.66 mm
	2:	1.39 mm	1.55 mm	1.43 mm
Mean composition		$Ca_{1.02}Mg_{0.89}Fe_{0.07}$	$Ca_{1.02}Mg_{0.91}Fe_{0.06}$	$Ca_{1.01}Mg_{0.90}Fe_{0.06}$
		$Al_{0.12}Si_{1.90}O_6$	$Al_{0.109}Si_{1.93}O_6$	$Al_{0.11}Si_{1.92}O_6$

FIGURE 2. Sample 1.1, electron-microprobe Al, Si, Mg, and Fe analytical profiles along the [100]* direction with analysis points every 7 μm, plus a general map of Al concentration in the same sample with analysis points every 50 μm.

coupled with Mg and Fe substitution. Aluminum and Si cations show variations with amplitude larger than Fe and Mg. Figure 2 shows that the core of the crystal is enriched in Al compared to the edge. In Figure 4, we show Al and Si profiles measured in the three samples for two different crystallographic directions. Variation of Al and Si are anti-correlated.

All crystals exhibit almost identical Al concentrations on edges (0.10–0.11 pfu), but Al at the core is different for the three crystals, with variations from 0.06 to 0.14 pfu. The Al concentration is a maximum at the core for sample 1.1 but a minimum for

sample 1.2, and almost homogeneous for sample 1.3.

It is interesting to note that the Al zoning observed in sample 1.1 along direction [100]* is not symmetric (Figs. 2 and 5). This asymmetry is probably due to the fact that during crystal growth, one of the (100) faces stopped earlier than the other faces [the larger (100) face is a natural as-grown face], and the true center of the crystal (its nucleation site) is located closer to this face (≈450 μm) than to the opposite edge (≈650 μm). If the results of the profile are folded at the level of this center they superpose almost exactly (Fig. 5). This observation demonstrates that main

TABLE 2. Ion microprobe, measurement of $\delta^{18}O$ on diopside crystal 1.2 from granulite facies marble, Adirondack Mountains, New York

Analysis no.	Position	$^{18}O/^{16}O$ raw (×10^{-3})	Distance from edge (µm)	$\delta^{18}O$ (‰) VSMOW	1σ (‰)
2	Std-core	2.062625	core	23.03	0.095
3	Std-core	2.062999	core	23.21	0.106
4	Std-core	2.062533	core	22.96	0.096
5	Std-core	2.062544	core	22.96	0.117
6	Std-core	2.062900	core	23.13	0.115
7	mantle	2.063326	170	23.33	0.134
8	mantle	2.063491	220	23.40	0.107
9	mantle	2.062800	270	23.05	0.110
10	Std-core	2.062472	core	22.88	0.119
11	Std-core	2.062976	core	23.12	0.106
12	Std-core	2.063012	core	23.13	0.114
13	mantle	2.063345	320	23.28	0.104
14	mantle	2.063337	380	23.27	0.095
15	mantle	2.063194	430	23.19	0.088
16	Std-core	2.062971	core	23.07	0.123
17	Std-core	2.062895	core	23.02	0.114
18	Std-core	2.062560	core	22.84	0.132
19	near core	2.063573	480	23.34	0.121
20	near core	2.063155	520	23.12	0.103
21	near core	2.062979	580	23.02	0.105
22	Std-core	2.063051	core	23.05	0.105
23	Std-core	2.063190	core	23.11	0.101
24	Std-core	2.062874	core	22.94	0.129
25	near core	2.063283	630	23.14	0.106
26	near core	2.063203	700	23.09	0.096
27	near core	2.063145	760	23.05	0.088
28	Std-core	2.063452	core	23.19	0.095
29	Std-core	2.063127	core	23.02	0.242
30	Std-core	2.063174	core	23.03	0.079
31	mantle	2.063344	180	23.11	0.081
32	mantle	2.063501	240	23.18	0.086
33	mantle	2.063762	290	23.30	0.094

FIGURE 3. $\delta^{18}O$ ion-microprobe analyses performed in crystal 1.2 with a spot diameter of about 15 µm. (**a**) Photo of analyzed area with analysis pits along the [001] direction; numbers indicate the order of analysis. Larger unlabeled spots correspond to early qualitative analytical tests. (**b**) $\delta^{18}O$ VSMOW as a function of distance to grain edge. Data are corrected for ~0.3‰ of drift over the period of analyses. Error bars (±1σ).

zoning observed at the core of the crystal corresponds to features preserved from growth history, and are not the result of further exchange of the crystal with its environment. The only possible effect of metamorphic annealing after crystal growth was to smooth the original zoning profile through diffusion.

Oxygen isotopes profile

Table 2 shows the results of ion-microprobe analyses performed along direction [001] in crystal 1.2. In Figure 3, $\delta^{18}O$ is shown for analyses along a [001] path from the edge of the crystal. The value of $\delta^{18}O$ in the core is within 0.2‰ of the mantle. This difference is less than the 2σ error of the measurements; we can consider this crystal to be homogeneous in $\delta^{18}O$ at least up to within 200 µm from its edge. There are no analyses in the outer 200 µm wide rim, which is inferred to show zoning due to post-metamorphic exchange (Edwards and Valley 1998). Contrary to electron-microprobe analyses of Al, the oxygen-isotope ratio is homogeneous within ±0.2‰ in the core and mantle of this Adirondack diopside.

Numerical modeling

We have shown that the Al concentration profiles observed in the diopside crystals are probably due to different growth histories
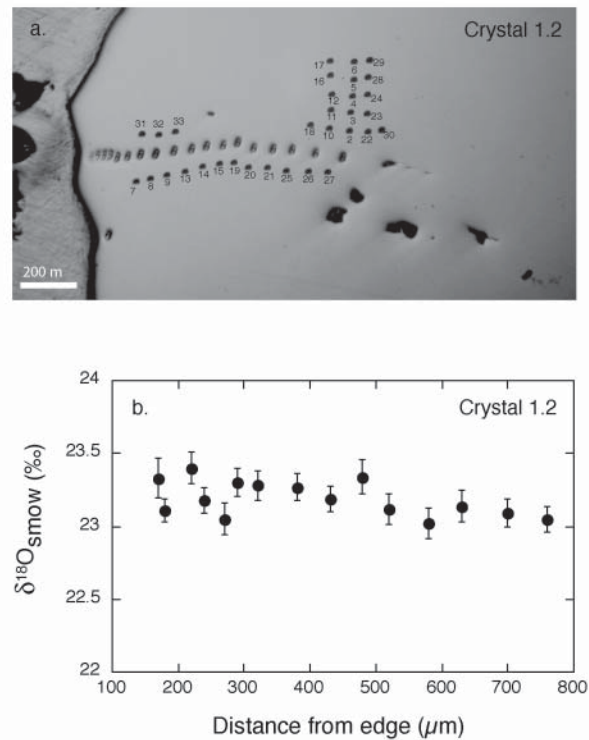
between cores and edges. The cores of the three crystals have different Al and Si concentrations, suggesting that they crystallized from slightly different bulk compositions in a heterogeneous sedimentary rock or that Al metasomatism was locally variable during crystal growth (Fig. 4). We know from previous studies that this rock underwent contact metamorphism at 1155 Ma followed ca. 100 Ma later by regional metamorphism at 770 ± 30 °C lasting ≈ 50 Ma. Assuming the shape of the Al profiles of the crystals prior to the regional metamorphism, and knowing the diffusion rate of Al-Si exchange in diopside, we can deduce the final shape of the profiles. We can calculate from these simulations the original shape of zoning that best fits the observed final profiles.

Modeling: assumptions and inputs

We used a one-dimension diffusion model and assumed that lateral diffusion has a minor effect on Al-diffusion profiles. The equation of one-dimensional diffusion for an element i with concentration (C) along direction x is given by:

$$\frac{\partial C_i(x,t)}{\partial t} = D_x \frac{\partial^2 C_i(x,t)}{\partial x^2} \tag{1}$$

D_x is the coefficient of diffusion along direction x, and is assumed to be independent of the variation of composition during diffusion. Solution of Equation 1 gives the concentration of element i as a function of position x and time t. The solution of the equation was fit using a finite-difference method with an
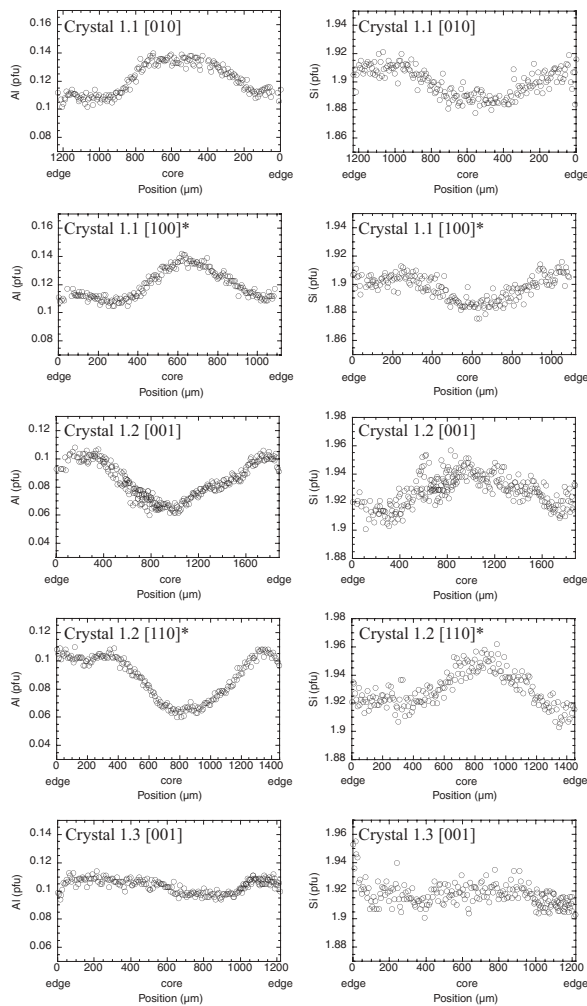
FIGURE 4. Electron-microprobe Al and Si profiles measured on crystals 1.1, 1.2, and 1.3.

FIGURE 5. Symmetry of Al concentration profiles in crystal 1.1 (**a**) Al profile along the direction [100] with its location in the crystal. (**b**) Symmetry of the profile observed when data are folded from the center of the crystal.

alternating directions implicit algorithm. This is a predicting-correcting method and it is equivalent to a Crank-Nicholson method (Yanenko 1968). We can deduce a final profile from any original distribution concentration of Al on which diffusion occurs during metamorphism. We tested two different original distributions: the first flat, and the second with a "top hat" shape.

The process controlling the evolution of the distribution of Al concentration is Al-Si inter-diffusion. We assume that the edge concentration is in equilibrium with the surrounding environment during granulite-facies metamorphism and is equal to the value given by electron-microprobe measurement (≈0.11 Al pfu). There is no temperature gradient in the crystal.

Original Al profiles

It was impossible to simulate the Al profiles observed in crystals 1.1 and 1.2 starting from a flat original Al distribution with concentration equal to the core concentration. However, Figure 6 shows that modeling of Al profiles in both directions is possible if we assume an original "top hat" step profile in the grains. The
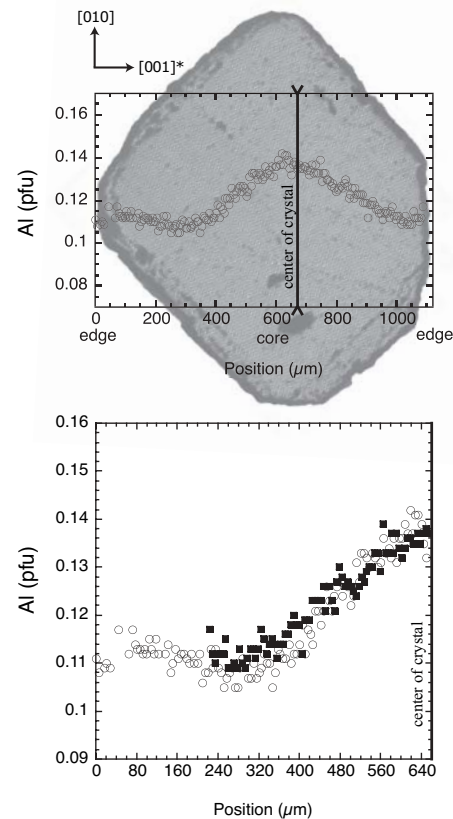
diffusion coefficient that best fits the observed profiles is 3.10^{-24} m^2/s, assuming that the granulite-facies event lasted for 50 Ma. It corresponds perfectly with the coefficient expected from extrapolation of experimental laws at 770 °C (Fig. 7). We also simulated the Al-diffusion profile due to the combination of metamorphism lasting for 50 Ma with a diffusion coefficient of 3.10^{-24} m^2/s followed by a cooling at 1 °C/Ma assuming an activation energy for the diffusion law equal to 211 kJ/mol (gray solid line, Fig. 6): the effect of cooling induces very little change in the final diffusion profile and its effect can be neglected. Starting with an initial profile smoother than a step shape profile would require a smaller diffusion coefficient in order to fit the measured Al profiles. This is quite unlikely since the diffusion coefficient used already falls within the lower extrapolation values of diffusion laws (see Fig. 7). Thus the results of simulations are consistent with the conclusion that the original Al zoning in diopside was sharp and corresponded to a rapid change of growth conditions. The difference of composition of original profiles suggests two steps of crystallization: (1) cores crystallized from different local environments (different Si or Al activities?) leading to different core compositions, and (2) an abrupt change in growth conditions of grains producing edges with homogeneous concentrations.

The simulations shown on Figure 6 invite an additional comment on the diffusion coefficients of Al-Si inter-diffusion in diopside: the profile measured in the direction [001] of crystal
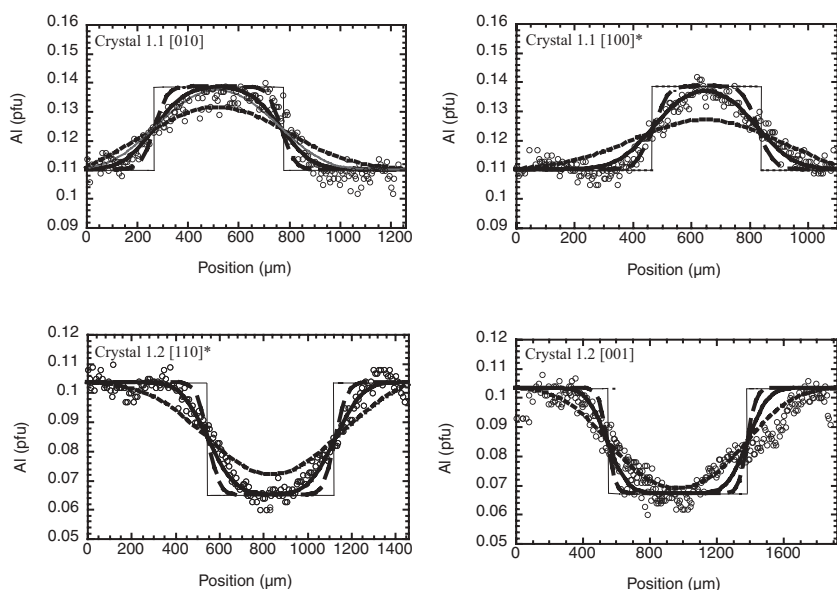
FIGURE 6. Modeling of the evolution of Al concentration profiles in crystals 1.1 and 1.2 after 50 Ma of regional metamorphism. Data (circles); initial "top hat" step profiles (thin solid lines); final profiles obtained for different diffusion coefficients: $1.5 \cdot 10^{-23}$ m^2/s (short dashed lines), $3 \cdot 10^{-24}$ m^2/s (thick solid lines), $1.5 \cdot 10^{-24}$ m^2/s (long dashed lines), $3 \cdot 10^{-24}$ m^2/s followed by a cooling at a rate of 1 °C/Ma (thin gray line in crystal 1.1 [010]).

1.2 is best fit with a diffusion coefficient slightly faster than for other directions (1.5×10^{-23} m^2/s). This result suggests that Al-Si inter-diffusion in diopside is anisotropic, the fastest diffusion occurring along the direction of silica chains.

DISCUSSION

Validity of the Al profiles modeling

The accuracy of the modeling has been tested by comparison with analytical solutions for simple geometries. A 1D model is a sufficient approximation to describe diffusion in these diopsides where the length of diffusion was short in relation to the crystal radius. We performed a 2D model using the same finite-elements approach as for the 1D model. In crystal 1.2, the Al-Si diffusion profile along the fast direction [001] ($1.5 \cdot 10^{-23}$ m^2/s) is similar to the profile for 1D modeling. The only difference is observed along the slow direction [110]* ($3 \cdot 10^{-24}$ m^2/s), where the profile is depressed by less than 0.002 Al pfu in the center of the crystal to follow the profile imposed by the fast direction. This small difference decreases progressively when we move away from the center and almost vanishes at 200 μm from the center. This difference is smaller than the scatter of data points. In crystal 1.1, a very small difference is observed, mainly due to the fact that the analyses were performed along the diagonal of the square shape of the crystal. Again, the differences are much smaller than the scatter of data.

For all profiles, the differences between 1D and 2D modeling do not change the estimation of diffusion coefficients. The contribution of the diffusion in the third direction will not notably modify these results.

It is also assumed in the model that the local high-T metamorphism due to the intrusion of the Mt. Marcy anorthosite at 1155 ± 5 Ma induced almost no diffusion profiles or negligible diffusion profile compared to the regional granulite-facies metamorphism. This is justified by the short duration after diopside growth during the shallow contact metamorphic event (McLelland et al. 1996).
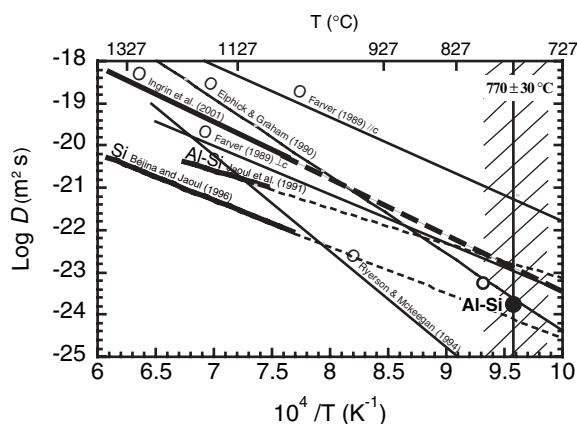

FIGURE 7. Diffusion coefficients of Si, Al-Si inter-diffusion and O self-diffusion and their extrapolations from Jaoul et al. (1991), Béjina and Jaoul (1996), Ingrin et al. (2001), Elphick and Graham (1990), Farver (1989), and Ryerson and McKeegan (1994). Full circle represents the Al-Si diffusion coefficient deduced from the modeling at the peak of metamorphism; empty circle is the estimate of the O diffusion coefficient from Sharp and Jenkin (1994).

The peak temperature of regional granulite-facies metamorphism is assumed to occur between 1090–1035 Ma, during Ottawan orogeny (McLelland et al. 2001). Duration of 50 Ma for the metamorphism is assumed, but this value may be considered an upper limit (Clechenko and Valley 2003). A shorter time at elevated temperature will only marginally affect the value of the diffusion coefficients used for the modeling of profiles. For instance, if peak temperatures of metamorphism lasted half as long (25 Ma), the model would yield diffusion coefficients a factor of two higher. This would not change the conclusions of the study. This effect is much smaller than the uncertainties of the diffusion coefficients deduced from the modeling or the extrapolations of experimental values.

Rates of diffusion and $\delta^{18}O$ homogeneity

The value of the diffusion coefficient obtained for the inter-diffusion of Al-Si ($3\cdot10^{-24}$ m^2/s) is in very good agreement with extrapolations of experimental data of Jaoul et al. (1991) and Béjina and Jaoul (1996) (Fig. 7). Extrapolation of experimental O-diffusion laws to 770 °C by Elphick and Graham (1990) and Ingrin et al. (2001) along any direction, and Farver (1989) perpendicular to [001] gives diffusion coefficients comparable to those of Al-Si interdiffusion while diffusion data by Ryerson and McKeegan (1994) predict much lower values (Fig. 7). Only the extrapolation of experimental data by Farver (1989) along [001] gives diffusion coefficients two orders of magnitude higher than coefficients of Al-Si inter-diffusion (Fig. 7). The possibility of an artifact in these latter data was previously discussed in Ingrin et al. (2001). The data of Farver were acquired in water-saturated conditions that are far from those prevailing in dry granulite-facies metamorphism ($a_{H_2O} \leq 0.14$; Johnson et al. 2002), which are believed to be closer to conditions of dry experiments like those performed by Ryerson and McKeegan (1994) and Ingrin et al. (2001). The low O-diffusion rate in diopside deduced from experiments agrees well with the empirical estimate of O-diffusion rate deduced by Sharp and Jenkin (1994) (Fig. 7). The effect of the Grenville metamorphism at 770 °C on any preexisting $\delta^{18}O$ gradient in the core of the crystal would have the same effect as for the Al-Si profiles; the total diffusion length of O during the peak of metamorphism would be less than 200 μm. Thus, we can conclude that the observed homogeneity in $\delta^{18}O$ was acquired during crystal growth and very probably little change occurred by exchange during dry granulite-facies metamorphism.

GEOLOGICAL IMPLICATIONS

Due to the complex polymetamorphic history of the Adirondacks, it is not surprising that diopsides recorded Al zoning prior to the high-grade Grenville metamorphism. The preservation of zoning from the early crystallization of diopsides allowed us to identify three different stages of evolution of the marble in relation to fluid infiltration: (1) crystallization of diopside cores with variable Al composition due to restricted fluid circulation or differing sedimentary composition; (2) pervasive fluid infiltration that crystallized the homogenous rims of diopsides; and (3) later smoothing of Al profiles during granulite-facies metamorphism. No significant change of $\delta^{18}O$ occurred during stages 1, 2, or 3. The abrupt change of diopside Al distribution between stage 1 and 2 suggests that the pervasive fluid infiltration was correlated with a rapid event probably during contact metamorphism linked to the anorthosite intrusion.

REFERENCES CITED

Béjina, F. and Jaoul, J. (1996) Silicon self-diffusion in quartz and diopside measured by nuclear microanalysis methods. Physics of the Earth and Planetary Interiors, 97, 145–162.

Bohlen, S.R. and Essene, E.J. (1978) Igneous pyroxenes from metamorphosed anorthosite Massifs. Contributions to Mineralogy and Petrology, 65, 433–442.

Bohlen, S.R., Valley, J.W., and Essene, E.J. (1985) Metamorphism in the Adirondacks I. Petrology, pressure, and temperature. Journal of Petrology, 26, 971–992.

Clechenko, C.C. and Valley, J.W. (2003) Oscillatory zoning in garnet from the Willsboro wollastonite skarn, Adirondack Mts, New York: a record of shallow hydrothermal processes preserved in a granulite facies terrane. Journal of Metamorphic Geology, 21, 771–784.

Dodson, M.H. (1973) Closure temperature in cooling geochronological and petrological systems. Contributions to Mineralogy and Petrology, 40, 259–274.

Edwards, K.J. and Valley, J.W. (1998) Oxygen isotope diffusion and zoning in diopside: The importance of water fugacity during cooling. Geochimica et Cosmochimica Acta, 62, 2265–2277.

Eiler, J.M., Baumgartner, L.P., and Valley, J.W. (1992) Intercrystalline stable isotope diffusion: a fast grain boundary model. Contributions to Mineralogy and Petrology, 112, 543–557.

Eiler, J.M., Valley, J.W., and Baumgartner, L.P. (1993) A new look at stable isotope thermometry. Geochimica et Cosmochimica Acta, 57, 2571–2583.

Eiler, J.M., Valley, J.W., Graham, C.M., and Baumgartner, L.P. (1995) Ion microprobe evidence for the mechanisms of stable isotope retrogression in high-grade metamorphic rocks. Contributions to Mineralogy and Petrology, 118, 365–378.

Elphick, S.C. and Graham, C.M. (1990) Hydrothermal oxygen diffusion in diopside at 1 Kb, 900–1200 °C, a comparison with oxygen diffusion in forsterite and constraints on oxygen isotope disequilibrium in peridotite nodules. Terra Abstract, 7, 72 (abstract).

Farver, J.R. (1989) Oxygen self-diffusion in diopside with application to cooling rate determinations. Earth and Planetary Science Letters, 92, 386–396.

Ingrin, J., Pacaud, L., and Jaoul, O. (2001) Anisotropy of oxygen diffusion in diopside. Earth and Planetary Science Letters, 192, 347–361.

Jaoul, O. and Béjina, F. (2005) Empirical determination of diffusion coefficients and geospeedometry. Geochimica et Cosmochimica Acta, 69, 1027–1040.

Jaoul, O., Sautter, V., and Abel, F. (1991) Nuclear microanalysis: a powerful tool for measuring low atomic diffusivity with mineralogical application. In J. Ganguly, Ed., Diffusion, Atomic ordering, and Mass Transport: Selected Topics in Geochemistry, 8, p. 198–220. Advances in Physical Geochemistry, Springer-Verlag, New York.

Johnson, E.J., Rossman, G.R., Dyar, M.D., and Valley, J.W. (2002) Correlation between OH concentration and oxygen isotope diffusion rate in diopsides from the Adirondack mountains New York. American Mineralogist, 87, 899–908.

Lasaga, A.C. (1983) Geospeedometry: an extension of geothermometry. In S.K. Saxena, Ed., Advances in physical geochemistry, kinetics and equilibrium in mineral reactions, p. 81–114. Springer, Heidelberg.

McLelland, J., Chiarenzelli, J., Whitney, P., and Isachsen, Y. (1988) U-Pb zircon geochronology of the Adirondack mountains and implications for their geologic evolution. Geology, 16, 920–924.

McLelland, J., Daly, J.S., and McLelland, J.M. (1996) The Grenville orogenic cycle (ca. 1350–1000 Ma): an Adirondack perspective. Tectonophysics, 265, 1–28.

McLelland, J., Hamilton, M.S., Selleck, B., McLelland, J., Walker, D., and Orrell, S. (2001) Zircon U-Pb geochronology of the Ottawan orogeny, Adirondack highlands, New York: regional and tectonic implications. Precambrian Research, 109, 39–72.

McLelland, J.M., Bickford, M.E., Hill, B.M., Clechenko, C.C., Valley, J.W., and Hamilton, M.A. (2004) Direct dating of Adirondack massif anorthosite by U-Pb SHRIMP analysis of igneous zircons: Implications for AMCG complexes. Geological Society of America Bulletin, 116, 1299–1317.

Mezger, K., Rawnsley, C.M., Bohlen, S.R., and Hanson, G.N. (1991) U-Pb garnet, sphene, monazite, and rutile ages: implications for the duration of high-grade metamorphism and cooling histories, Adirondack Mts. New York. Journal of Geology, 99, 415–428.

Pacaud, L., Ingrin, J., and Jaoul, O. (1999) High temperature diffusion of oxygen in synthetic diopside measured by nuclear reaction analysis. Mineralogical Magazine, 63, 673–686.

Ryerson, F.J. and McKeegan, K.D. (1994) Determination of oxygen self-diffusion in akermanite, anorthite, diopside and spinel: Implication for oxygen isotopic anomalies and the thermal histories of Ca-Al-rich inclusions. Geochimica et Cosmochimica Acta, 58, 3713–3734.

Sharp, Z.D. and Jenkin, G.R.T. (1994) An estimate of the diffusion rate of oxygen in diopside. Journal of Metamorphic Geology, 12, 89–97.

Valley, J.W. (2001) Stable isotope thermometry at high temperature In J.W. Valley and D.R. Cole, Eds., Stable isotope geochemistry, 43, p. 365–414. Reviews in Mineralogy, Mineralogical Society of America, Chantilly, Virginia.

Valley, J.W. and Essene, E.J. (1980) Akermanite in the Cascade Slide xenolith and its significance for regional metamorphism in the Adirondacks. Contributions to Mineralogy and Petrology, 74, 143–152.

Yanenko, N.N. (1968) Méthode à pas fractionnaires: résolutions de problèmes polydimensionnels de physique mathématique. Translated by P.A. Nepomiastchy. A. Colin, Ed., collection Intersciences (Paris); 205 p.